Catch Effect of Debris Flow for the Open Type Steel Check Dam by 3-Dimentional Analysis

Nobutaka Ishikawa[1], Gakuto Fukawa[2], Satoshi Katsuki[3] and Tadashi Yamada[4]

ABSTRACT

This paper presents a computer simulation approach on the catch effect of debris flow for an open type steel check dam by the 3-dimentional distinct element method(3-D DEM). First, the 3-D DEM is developed in order to examine the catch effect of debris flow for an open type steel check dam. Second, the hydrodynamic test is performed to investigate the catch effect of the debris flow for a model check dam. Finally, a computer simulation by the proposed 3-D DEM is carried out in order to compare with the hydrodynamic test results and the catch effect is confirmed by the beam slit interval of a steel check dam.
Key words: 3-D DEM, Steel check dam, Debris flow, Slit interval

INTRODUCTION

Fig.1 Open type steel check dam

Recently many steel check dams have been constructed in the mountainous areas in Japan as shown in **Fig.1**. This type structure is composed of steel pipes framed as a grid and it can flow soil and small gravels through the slit interval into the downstream, but it can prevent the large rocks in the debris flow by local and global deformation of steel pipes. Generally, a slit interval of beam seems to be 1.5 times (Steel Sabo Structure Committee,2001) of the largest diameter of rock and then the dam can catch the debris flow by interlocking gravels. This

1Professor Emeritus, National Defense Academy, Research Adviser, Society for the Study of Steel Sabo Structures, 2-7-5 Hirakawa-cho,Chiyoda-ku,Tokyo
102-0093,Japan (Tel: 81-3-5215-8228; Fax: 81-3-5215-8229; email: cgishikawa@m4.dion.ne.jp)
2 Civil Engineer , Naha Defense Facilities Administration Bureau Government of Japan, 3-25-1 Maejima Naha,Japan
3 Professor, Dept.of Civil Engineering, National Defense Academy, 1-10-20 Hashirimizu, Yokosuka 239-8686,Japan
4 Professor, Dept. of Civil Engineering, Chuo University, 1-13-27 Kasuga, Tokyo 112-8551,Japan

criteria is based on the hydraulic test for a concrete model check dam(Ikeya and Uehara,1980) and it is also verified by the 2-D DEM(Fukawa et.al, 2002). Although the grid type steel check dam has been examined by an experimental work (Mizuyama et.al, 1988), the catch effect of debris flow has not been investigated so far by the 3-dimentional analysis. Therefore, the 3-D DEM is first developed by extending the 2-D DEM (Fukawa et.al, 2002) Then, the hydrodynamic test is performed to examine the catch effect of debris flow by using a model apparatus. Finally, a computer simulation is executed to confirm the catch effect of debris flow by comparing with the model test results.

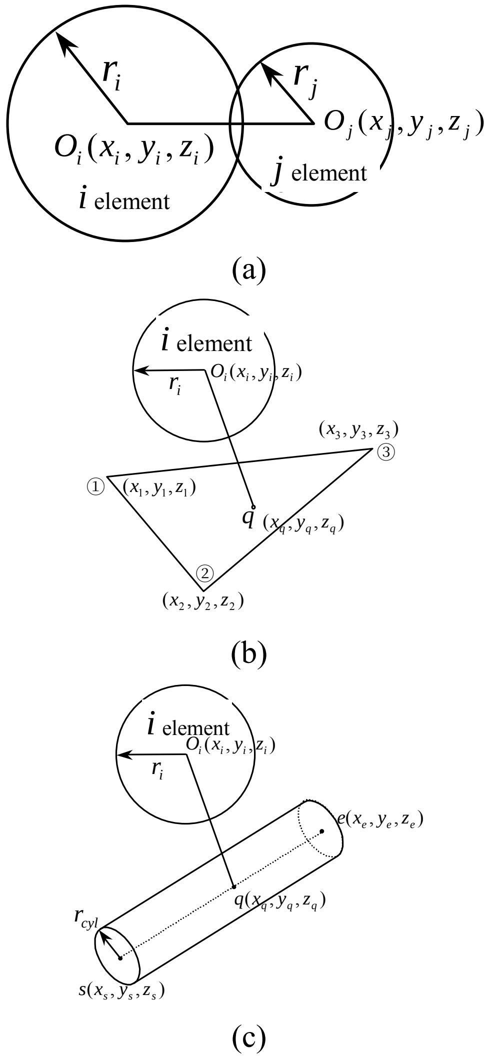

Fig.2 Contact decision

THE 3-DIMENTIONAL DISTINCT ELEMENT METHOD (3-D DEM)

The 3-D DEM is developed in order to examine the catch effect of debris flow by expressing a riverbed into a plane element, a grid check dam into cylindrical elements and a rock into a sphere element.

Contact Decision

The contact decision between 2 sphere elements is performed as the following equation as shown in **Fig.2**(a).

$$D_{ij} \le r_i + r_j \tag{1a}$$

where, D_{ij} is the distance between i and j elements,

$$D_{ij} = \sqrt{(x_i - x_j)^2 + (y_i - y_j)^2 + (z_i - z_j)^2} \tag{1b}$$

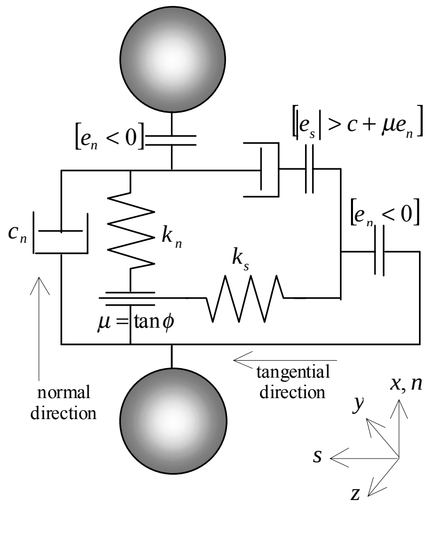

Fig.3 Contact force

x_i, y_i, z_i are the central coordinates of i element, x_j, y_j, z_j are the central coordinates of j element, r_i, r_j are the radius of i and j elements, respectively.

The contact between sphere and plane elements is decided by the following equation as shown in **Fig.2**(b)

$$D_p < r_i \qquad (1c)$$

where, D_p is the distance between i sphere element and a plane element.

The contact between a sphere element and a cylindrical element is judged by the following equation as shown in **Fig.2**(c).

$$D_{cy} \leq r_i + r_{cyl} \qquad (1d)$$

where, D_{cy} is the distance between a sphere element and a cylindrical element, r_{cyl} is the radius of a cylindrical element.

Contact Force

The contact forces at normal and tangential directions in the local coordinate as shown in **Fig.3** are formulated as follows ;

$$f_n = \bar{f}_n + k_n \Delta d_n + c_n \Delta d_n / \Delta t \qquad if \quad f_n \geq 0 \qquad (2a)$$

$$f_s = \bar{f}_s + k_s \Delta d_s + c_s \Delta d_s / \Delta t \qquad if \ |f_s| \leq c + \mu f_n \qquad (2b)$$

where, $\overline{f}_n, \overline{f}_s$ are the contact forces at normal and tangential directions in local coordinate at previous step, respectively, c is the cohesive force due to Mohr-Coulomb's Equation, c_n, c_s are the normal and tangential damping coefficients, k_n, k_s are the normal and tangential spring constants, respectively, μ is the dynamic friction coefficient, $\Delta d_n, \Delta d_s$ are the deformation increments of normal and tangential directions, respectively.

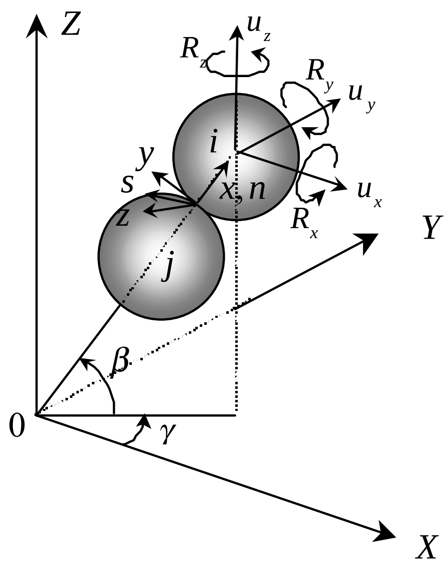

Fig.4 Global and local coordinates

These contact forces are transformed into the spring force acting each element as follows;

$$\mathbf{F}_{Bi} = \mathbf{B}_i^T \mathbf{T}_i^T \mathbf{f}_{ij} \qquad (3)$$

where, $\mathbf{F}_{Bi}$ is the spring force vector at I element, $\mathbf{f}_{ij}$ is the contact force vector at the local coordinate between i and j elements, $\mathbf{B}_i$ is the compatibility matrix of i element at the local coordinate, $\mathbf{T}_i$ is the transformation matrix from global to local coordinates as shown in Fig.4 as follows;

$$\mathbf{T}_i = \begin{bmatrix} \cos\gamma\cos\beta & \sin\gamma\cos\beta & -\sin\beta \\ -\sin\gamma & \cos\gamma & \\ \cos\gamma\sin\beta & \sin\gamma\sin\beta & \cos\beta \end{bmatrix} \tag{4}$$

in which, $\gamma = \tan^{-1}\{(y_i - y_j)/(x_i - x_j)\}$, $\beta = \tan^{-1}\left\{(z_i - z_j)/\sqrt{(x_i - x_j)^2 + (y_i - y_j)^2}\right\}$

Fluid Force

The fluid force acting a gravel element is expressed as follows;

$$F_w = \frac{1}{2} C_D \rho A_i |U - v|(U - v) \tag{5}$$

where, F_w is fluid force, C_D is the resistant coefficient, A_i is the projecting area to the stream direction of a gravel element, U is water velocity, ρ is water density, v is gravel velocity.

Equation of Motion

The acceleration of a gravel element is found from the Newton's law as follows;

$$\ddot{\mathbf{u}}_t = \mathbf{m}_i^{-1} \left[\sum \mathbf{F}_{Bi} + \mathbf{F}_w \right] \tag{6}$$

where, $\ddot{\mathbf{u}}_t$ is the acceleration vector of a gravel element, $\mathbf{m}_i$ is the mass matrix of i element, $\sum$ is the integral of contact elements, $\mathbf{F}_w$ is the fluid force vector.

Then, the velocity and deformation are given as follows;

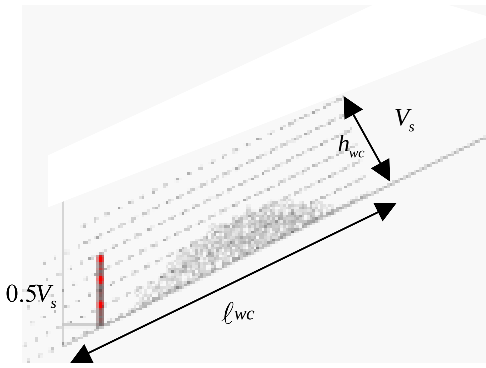

Fig.5 Fluid velocity model

$$\dot{u}_{t+\Delta t} = \dot{u}_t + \ddot{u}\Delta t \tag{7a}$$

$$u_{t+\Delta t} = u_t + \left(\frac{\dot{u}_{t+\Delta t} + \dot{u}_t}{2}\right)\Delta t \tag{7b}$$

Flow Velocity Model

Although the flow velocity changes practically due to the interaction of gravel elements, herein, it is modeled as shown in **Fig.5**. That is, the constant velocity V_s is given to the last gravel and the constant velocity $0.5V_s$ is provided for the head gravel. It is assumed that the velocity is decreased proportionally to the distance from the last gravel and the gravel velocity at the higher position in some distance is larger than one at the waterbed.

HYDRODYNA MIC MODEL TEST

Outline of Test

In order to examine the catch effect of debris flow, the hydrodynamic test is carried out by using the transparent acrylic waterway in which the length is 3m, the width is 0.2m, the depth is 0.3m and the waterbed slope is 20° as shown in **Fig.6**. The debris flow is composed of 4 kinds of gravel (diameter is made of 5, 10, 15, 20mm) and flow water with 2.7ℓ/sec or 3.4ℓ/sec. The open type check dam is modeled as shown in **Fig.7** in which the interval of column is fixed as 2.25 times of the maximum diameter of gravel and the interval of beam is changed as 1.5-2.5 times of the maximum diameter of gravel. The 11 test cases were performed including the case without beam as shown in **Table 1**.

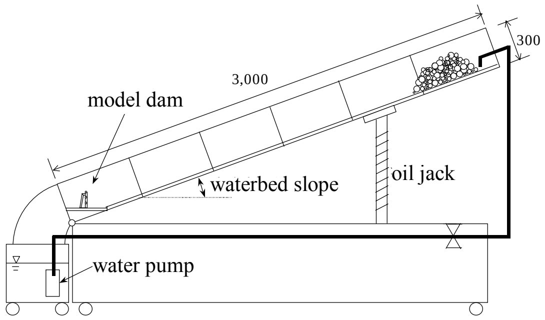

Fig. 6 Hydrodynamic test

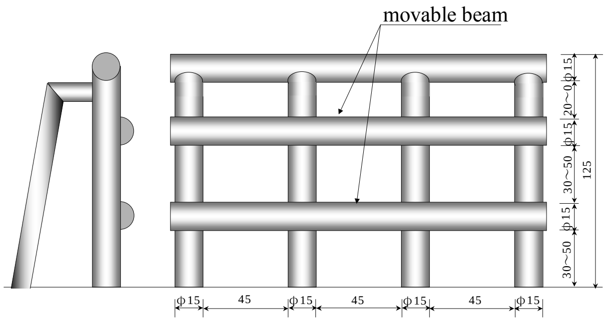

Fig.7 Open type model check dam

Table 1 Test case

No	interval	ℓ / d_{max}	flow water	slope
None-1	none		3.4ℓ/s	20°
150-1	30mm	1.5		
150-2				
150-3				
150-4			2.7 ℓ /s	15°
200-1	40mm	2	3.4 ℓ /s	20°
200-2			2.7 ℓ /s	
225-1	45mm	2.25		
225-2				
250-1	50mm	2.5		
250-2				

Test Results and Considerations

Figure 8 shows the catch condition of debris flow in the case of beam interval with ℓ/d_{max}=1.5 changing at the time interval 0.2 sec from t=1.8sec to t=2.6sec. It is found that the debris flow is blocked by the check dam at t=2.2sec and some gravels are overflowed into the downstream at t=2.4-2.6sec.

Figure 9 illustrates the catch state of debris flow in the case without beam.
It is noted that the dam has once caught debris flow at t=2.2sec, but it cannot block most of gravels due to continuing flow at t=3.0sec, because beams are removed from the dam.

(a)t=1.8sec

(b)t=2.0sec

(c)t=2.2sec

(d)t=2.4sec

(e)t=2.6sec

Fig.8 Catch process by test （ℓ / d_{max} =1.5）

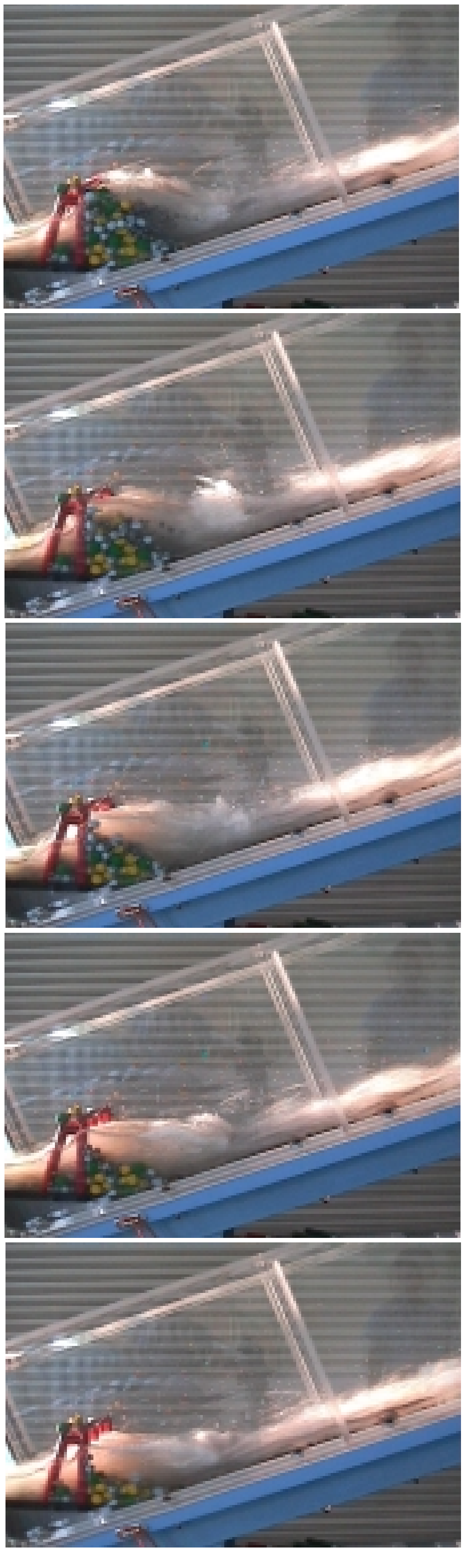

(a)t=2.2sec

(b)t=2.4sec

(c)t=2.6sec

(d)t=2.8sec

(e)t=3.0sec

Fig.9 Catch process by test （without beam）

(a) ℓ / d_{max} =1.5

(b) ℓ / d_{max} =2.0

(c) ℓ / d_{max} =2.25

(d) ℓ / d_{max} =2.5

Fig.10 Final catch state by model test

Figure10 expresses the final catch states of debris flow at the beam interval ℓ/d_{max} =1.5,

Table 2 Input data

Item		value	remark
Slope θ		20 °	
Velocity U	No dam	200cm/s	
	Dam	300cm/s	
Resistant coefficient C_D		0.49	
Unit volume weight ρ		$1.9g/cm^3$	
Min. weight m_{min}		$0.156g/\ cm^3$	
Max. weight m_{max}		$10.45\ g/\ cm^3$	
Total element		3,000	
Time interval		$\Delta t = 1.0\times10^{-5}$	
Spring constant	Normal k_n	1.0×10^3 kN/ cm	
	Tangential k_s	4.0×10^2 kN/ cm	
Damping coefficient	Normal c_n	1.13-9.06	Depend on size
	Tangential c_s	0.358-2.86	Depend on size
Friction coefficient μ		1.0	
Cohesive force c	No dam	0.0	
	Dam	1.0	
Repulsion coefficient e		1.0	

2.0,2.25, 2.5. It is confirmed that the dam can block most of gravels in cases of ℓ/d_{max} =1.5, 2.0, 2.25, but the gravel volume caught in the case of ℓ/d_{max}=2.5 is less than one in the cases of ℓ/d_{max}=1.5, 2.0, 2.25

Computer Simulation and Considerations

Computational Condition

The parameters used in the analysis are shown in **Table 2**. Herein, the resistance coefficient C_D=0.49 is adopted within the range of the Reynolds's number $R_e=1.3x10^4\sim3.2x10^4$. The time interval $\Delta t=1.0x10^{-5}$sec is given so that the emission may not occur in the solution process of equation of motion. The damping coefficients of normal and tangential directions are different by the diameter of gravels. The friction coefficient μ=1.0 was determined by a simple slide test.

Catch Process (beam interval ℓ/d_{max}=1.5)

Figure 11 shows the computational process in the case of beam interval ℓ/d_{max}=1.5. It is found that the head of debris flow is arrived in the front of dam at the time t=2.1sec, and is dammed up by the steel grid at the time t=2.2sec. A part of gravels have climbed over and flowed through the steel grid to the downstream. However, an outflow is stopped from intermediate grid at the time t=2.3sec and the dam is completely blocked with gravels at the

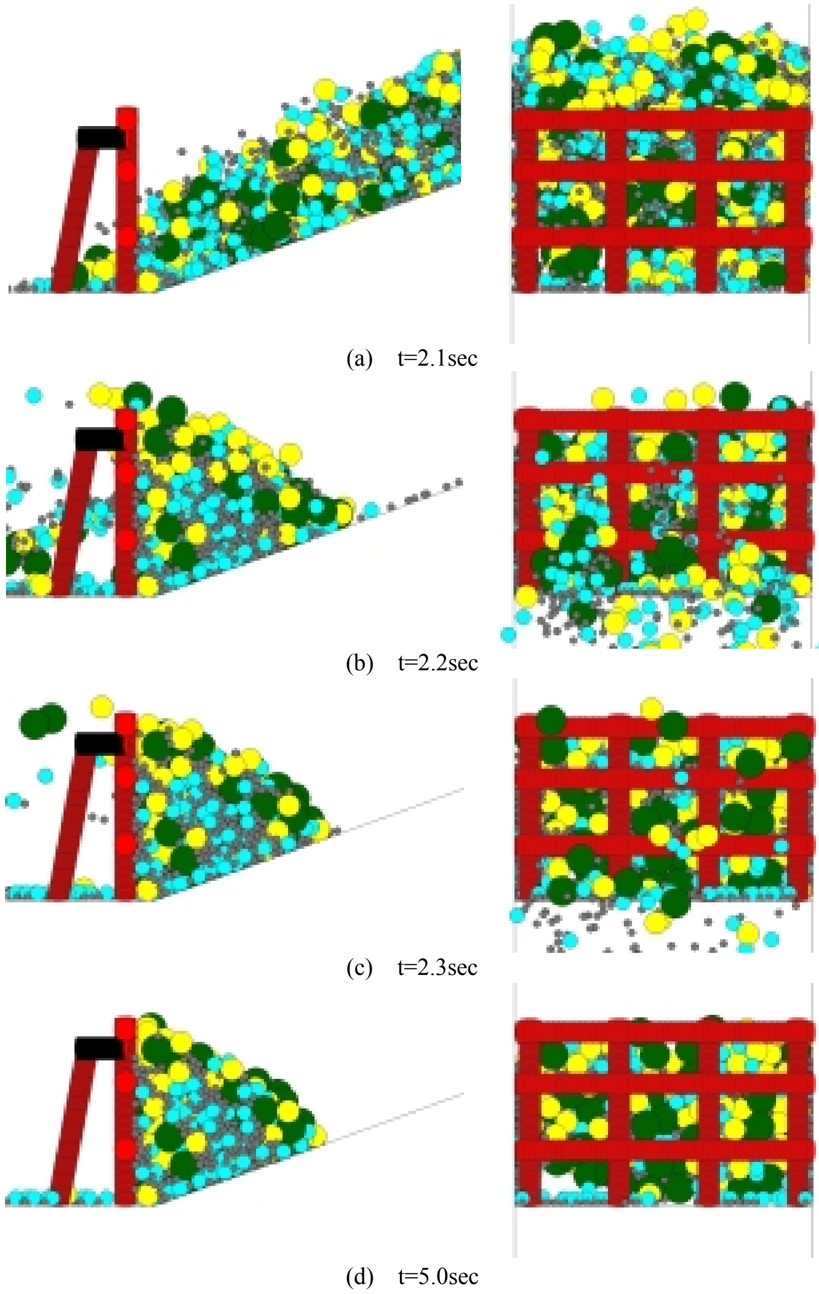

side view front view

Fig.11 Catch process by analysis (beam interval ℓ / d_{max} =1.5)

time t=5.0sec. These catch processes are quite similar to the test results of **Fig.8** (a)-(d). It is also recognized from the front face of **Fig.10** (d) that the open part of grid is dammed up by interlocking gravels each other.

Catch Process (without beam)

Figure 12 illustrates the case without beam. It is noted that the head of gravels is reached at the front of dam on time t=2.1sec in which the start condition coincides with the case of beam interval ℓ/d_{max}=1.5. At the time t=2.2sec the gravels were once intercepted by four steel columns, but all particles are washed away to the lower stream at the time t=2.3-5.0 sec. These processes are good agreement with those of **Fig.9**.

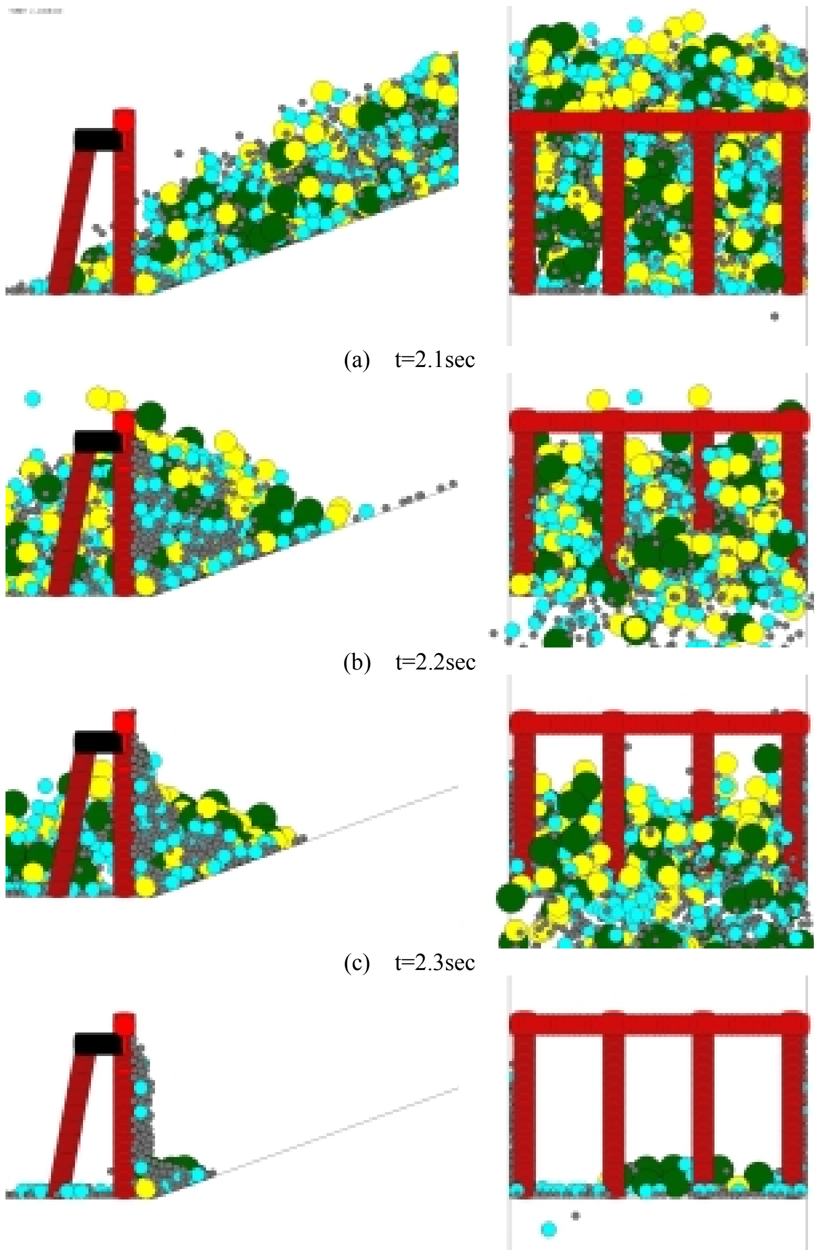

(a) t=2.1sec

(b) t=2.2sec

(c) t=2.3sec

(e) t=5.0sec

side view front view

Fig.12 Catch process by analysis (without beam)

Comparison with Test Results

Figures 13 and 14 express the relations between catch rates of particle number and volume versus the beam interval comparing with the test results. It should be noted that the catch rate of particle number is decreased with the increase of beam interval and the analysis results are relatively good agreement with the test results. It is also given that the catch rate of particle volume is decreasing as the increase of beam interval. Generally speaking, this computational method can estimate well the catch rates of number and volume of gravels for the cases of various beam intervals.

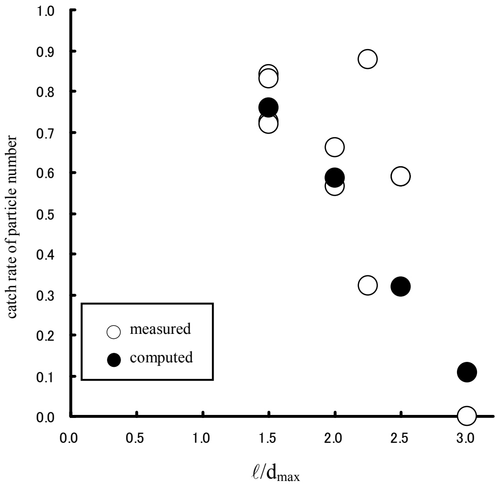

Fig.13 Catch rate of particle No. vs. ℓ/d_{max}

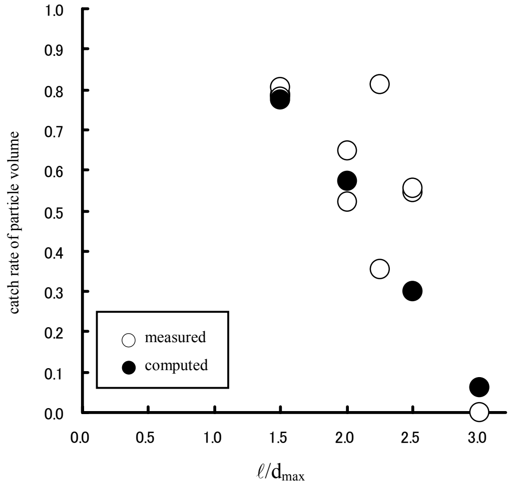

Fig.14 Catch rate of volume vs. ℓ/d_{max}

Conclusions

The following conclusions are drawn from this study.

(1) The 3-dimentional distinct element method has been proposed in order to examine the catch effect of debris flow for the steel grid type check dam.

(2)As the hydrodynamic test results, it was found that the grid type check dam can catch the gravels in the case of beam interval ℓ/d_{max} =1.5.
However, the dam cannot catch gravels completely in the case without beam.

(3)The computational results are relatively good agreements with the test results from both viewpoints of catch rates of particle number and mass of gravels.

(4)Therefore, this 3-dimentional analysis can estimate the catch effect of debris flow for the open slit type of check dam.

References

Ikeya,H. and Uehara,S. (1980) An Experimental Study on the Effect of Debris Flow of Slit Sabo Dam, J. of JSECE,Vol.32, No.3,114,pp.37-44(in Japanese)

Mizuyama ,T., Suzuki,H., Oikawa,Y. and Morita, A. (1988) An Experimental Study on Open Type Sit Sabo Dam, J. of JSECE, Vol.41,No.2,pp.21-25(in Japanese)

Steel Sabo Structure Committee (2001) Design Manual of Steel Sabo Dam, pp.33-34(in Japanese)

Fukawa,G., Katsuki,S., Ishikawa,N., and Yamada,T.(2002) Simulation and Stochastic Evaluation of the Open Type Steel Check Dam for Damming Up Performance, INTERPRAEVENT 2002 In the Pacific Rim-Matsumoto/Japan, Vol.2,pp.751-760